Arab J Sci Eng (2016) 41:2751–2770
DOI 10.1007/s13369-016-2186-3

RESEARCH ARTICLE - PETROLEUM ENGINEERING

Modeling of Two-Phase Relative Permeability in Cambrian and Early Miocene Sandstone Reservoirs: A Case Study, Egypt

Mohamed S. El Sharawy[1]

Received: 16 April 2015 / Accepted: 11 May 2016 / Published online: 28 May 2016

Abstract The relative permeability is the ratio of the effective permeability to the absolute permeability. Due to the importance of relative permeability in reservoir simulation, there is a dominant need to upscale it. So, several models were introduced to modeling the relative permeability. Some correlation models were dependent on capillary pressure measurements, while other models did not require such measurements. In this study, four relative permeability correlation models were chosen to apply them on two sandstone reservoir (labeled A and B) data sets. The two reservoirs belong to different ages and depositional environments. Both reservoirs are located in the Southern Gulf of Suez, Egypt. Reservoir A is the Nubian sandstone of Cambrian age. Reservoir B is the Nukhul clastic of Early Miocene age. The data sets include laboratory measurements of unsteady-state gas–oil relative permeability and steady-state water–oil relative permeability tests. The results indicate that the practical and modified Corey models were the most applicable model for the studied reservoirs. Additionally, prediction of relative permeability at saturation end points was carried out based on using routine core porosity and permeability by introducing new empirical equations. The relative permeability was used to identify rock wettability, water cut, water cutoffs and the areal and vertical sweep efficiencies.

Keywords Relative permeability · Wettability · Mobility ratio · Water cut

✉ Mohamed S. El Sharawy
sharawy2001@hotmail.com

[1] Geophysical Sciences Department- Room 405 – Physics Building, National Research Centre, El Behouth St., Dokki, Cairo, Egypt

List of Symbols

A, B, L and M	Positive numbers
E_{ABT}	Efficiency at breakthrough
E_D	Displacement efficiency
E_R	Overall waterflood oil-recovery efficiency
E_v	Vertical efficiency
f_w	The fractional flow of water (water cut)
k_{rg}	Relative permeability to gas
$k_{rg}@S_{org}$	Relative permeability to gas at residual oil Saturation in gas–oil system
k_{rnw}	Relative permeability for nonwetting phase
k_{rog}	Relative permeability to oil in the two phase Gas–oil system
k_{row}	Relative permeability to oil in the two phase Oil–water system
$k_{ro}@S_{wc}$	Relative permeability to oil at connate water saturation
$k_{ro}@S_{gc}$	Relative permeability to oil at critical gas saturation
k^*_{ro}	Normalized relative permeability to oil
k_{rw}	Relative permeability for wetting phase
$k_{rw}@S_{orw}$	Relative permeability to oil at residual oil saturation
k^*_{rw}	Normalized relative permeability to water
M	The mobility ratio
M_w	The molecular weight
no, nw, ng, ngo	□ Exponents on relative permeability curves
P	The pressure, psi
P_b	Rhe bubble—point pressure, psi
P_c	Capillary pressure, psi
P_d	Displacement pressure, psi
R_g	The normalized saturation

R_s The solubility of the gas–oil ratio, SCF/STB
S The salinity (%)
S_g □ Gas saturation
S_{gc} □ Critical gas saturation
S_o Oil saturation

Nomenclature

S_{oe} Normalized wetting phase saturation
S_{or} Residual oil saturation
S_{org} □ Residual oil saturation in the gas–oil system
S_{orw} Residual oil saturation in the water–oil system
S_w Water or wetting phase saturation
S_{w*} Normalized water saturation
S_{wc} □ (Irreducible) water saturation
S_{wir} Irreducible water saturation
T Temperature (°F)
V Permeability variation
μ_o The oil viscosity (cp)
μ_{obd} The dead oil viscosity above bubble point pressure (cp)
μ_{od} The dead oil viscosity (cp)
μ_w The water viscosity (cp)
μ_{w1} The water viscosity at atmospheric pressure and reservoir temperature (cp)
γg The specific gas gravity
ρ_o The oil density (API)

1 Introduction

The relative permeability of a fluid flowing in a porous medium is the ratio of its effective permeability to the absolute permeability of the porous medium. Relative permeability data are usually represented graphically in plots called relative permeability curves. Such curves could be for oil–water, oil–gas or gas–water systems. Figure 1 illustrates a relative permeability curve for oil–water system and its relation with the capillary pressure. The figure explains the main reservoir zones as well as the main used symbols in the relative permeability curves. According to several authors [1–7], the relative permeability is a function of numerous factors, such as saturation state, wettability, rock properties, pore size distribution, temperature and viscosity. Amyx et al. [2] stated that the relative permeability data can be used to:

- Model a particular process, for example fractional flow, fluid distributions, recovery and predictions
- Determine the free water surface, i.e., the level of zero capillary pressure or the level below which fluid production is 100 % water.
- Determine the residual fluid saturations.
- Aid in evaluating drill-stem and production tests.
- Determine the fluid distributions.
- Make future predictions for all types of oil reservoirs, where two-phase flow is involved.

Sources of the relative permeability can be categorized in the following three methods:

1. Production field data measurements,
2. Laboratory measurements include steady- and unsteady-state methods, capillary pressure method and centrifuge method and
3. Correlation models.

More details about these methods concerning preparations, conditions, procedures and techniques can be found in several textbooks such as [3,5].

In this study, we used the laboratory measurements of relative permeability for two sandstone reservoirs, belonging to different geologic and sedimentary basins, to upscale the relative permeability, as well as to determine some reservoir fluid properties. The first reservoir (reservoir A) is the Nubia sandstone. This reservoir is considered as one of the main reservoirs in the Gulf of Suez. It produced oil from several fields distributed throughout the Gulf of Suez. The Nubia sandstone, which overlies unconformably on basement, is composed mainly of sandstone intercalated by some streaks of shale and is ranged in age from Cambrian to Early Cretaceous. However, in the Southern Gulf of Suez, the Nubia sediments are dominantly Cambrian. Such sediments are believed to be deposited in a continental to fluvial braided conditions. The Nubia sandstone reservoir is ranged from poor to high quality depending on the degree of post-depositional diagenesis processes. The routine core analyses of several plugs obtained from four bore holes in the Southern Gulf of Suez indicate a heterogeneous reservoir with an average permeability value of 81 md. The helium porosity is ranged from 1.2 to 22 with an average value of 13.1.

The second reservoir (reservoir B) represented the lower member of the Lower Miocene Nukhul Formation. This member, Shoab Ali Member, is occurred only in the Southern Gulf of Suez and is composed mainly of sandstone intercalated by shale. It is probably deposited in fluviatile environment. The routine core analysis of one bore hole indicates an average permeability value of 1036 md. The helium porosity ranged from 2.1 to 22.9 with an average value of 16.8. The average grain density is 2.656 g/cc. The lithology description indicates cemented sandstone of light gray, fine to medium grains, with traces of mica, glauconite and iron oxide.

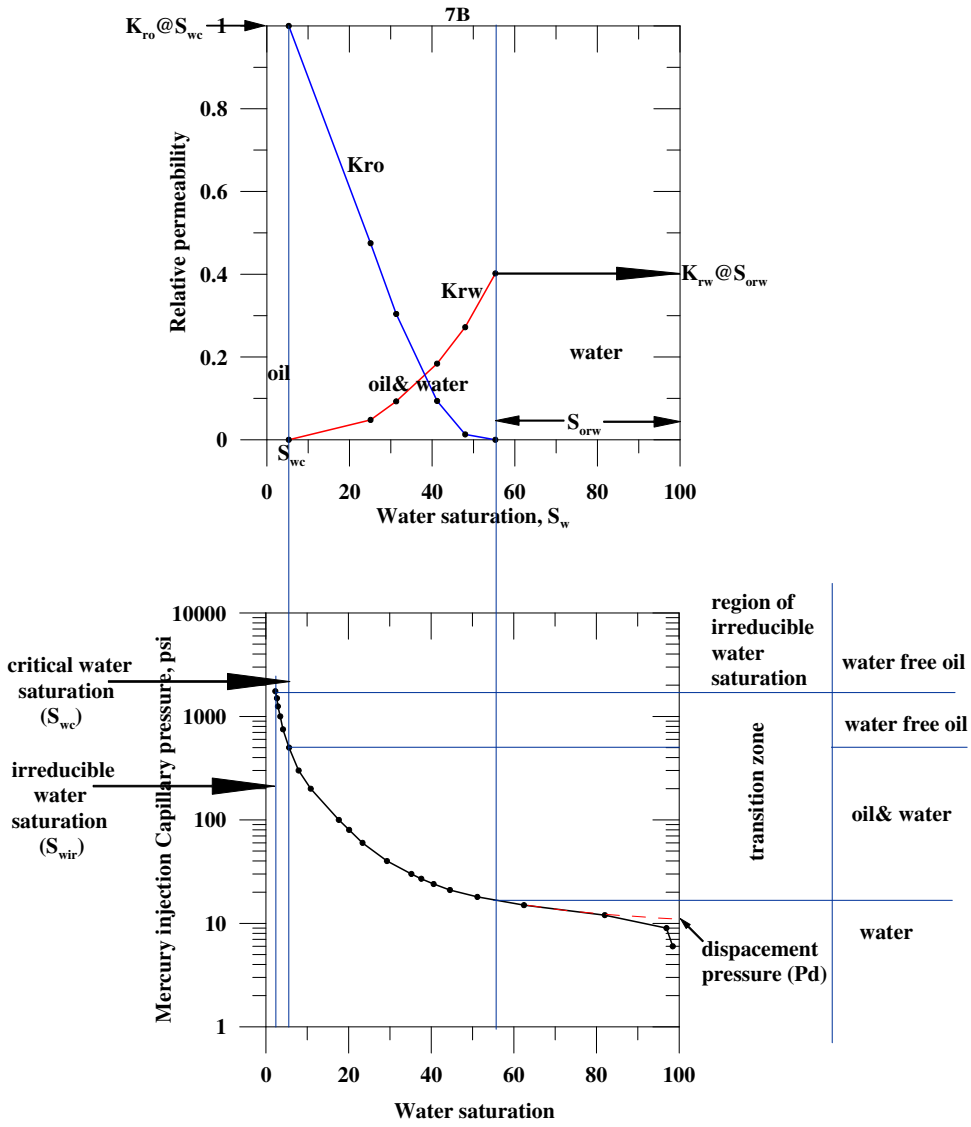

Fig. 1 Relationship between relative permeability and capillary pressure

2 Data and Methods

Two data sets were available for two different reservoirs used in this study. The first data set contains three core samples for unsteady-state gas–oil and steady-state water–oil systems for the reservoir "A." Three samples, two inches in diameter, were drilled from the preserved core material using refined mineral oil as the bit coolant. These samples were prepared for fresh-state relative permeability testing. Upon completion of this testing, the samples underwent Dean–Stark analysis by which the initial water saturation can be determined, and basic properties were measured at 200 and 2000 psi overburden pressure. The three samples were labeled 1B, 4B and 7B. The second data set includes five core samples for unsteady-state gas–oil system and steady-state water–oil system for the reservoir "B." The five samples, 1 inch in diameter, were drilled from the preserved core material using refined mineral oil as the bit coolant. These samples were prepared for fresh-state relative permeability testing. The samples were first flushed to remove water and replace the crude oil. The samples were then flushed under 450 psi back pressure using 17-cp mineral oil drive the samples to connate water saturation (S_{cw}). Following the relative permeability testing, the samples underwent Dean–Stark analysis, and basic properties were measured at 200 and 1500 psi effective overburden pressure. These samples were labeled 3D, 4D, 5D, 6D and 7D. Additional routine and special core data analyses as well as repeat formation tester (RFT) log were used for interpretation and calculation purposes. The petrophysical properties of the core samples are presented in Table 1.

Table 1 Petrophysical properties of the studied plugs and terminal fluids saturation

Sample no.	Pressure (psi)	Porosity	Air permeability (md)	Grain density (g/cc)	Diameter in inch	S_{org}	S_{orw}	S_{wir}
1B	200	0.147	28.9	2.64	2	20	33.4	4.6
	2000	0.143	24	2.64				
4B	200	0.132	12.5	2.64	2	19.7	24.5	3.8
	2000	0.126	10.6	2.64				
7B	200	0.174	101	2.64	2	28.7	44.7	5.3
	2000	0.17	76.9	2.64				
3D	200	0.162	436	2.63	1	24.1	45.7	4.5
	1500	0.156	400	2.63				
4D	200	0.152	64.7	2.68	1	17.5	46.9	6.8
	1500	0.149	60.4	2.68				
5D	200	0.204	1440	2.66	1	29.6	41.2	6.7
	1500	0.198	1420	2.66				
6D	200	0.242	1700	2.64	1	31.3	33.5	7
	1500	0.229	1540	2.64				
7D	200	0.2	912	2.66	1	27.9	32.3	9.2
	1500	0.194	877	2.66				

2.1 Unsteady-State Gas–Oil Relative Permeability Test

Relative permeability data can be obtained with unsteady-state methods very quickly because they do not require the attainment of equilibrium in the displacement process. So, many relative permeability data can be acquired in a few hours. In a typical unsteady-state method, the in situ fluids are displaced by injection of the displacing fluid at a constant rate or pressure, while measuring the produced fluids continuously. In designing experiments to determine relative permeability by the unsteady-state method, the following cautions must be taken into consideration [3]:

1. The pressure must be large enough to minimize the effect of capillary pressure.
2. The pressure differential across the core must be sufficiently small compared with total operating pressure so that compressibility effects are insignificant.
3. The core must be homogeneous.
4. The driving force and fluid properties should be held constant during the test.

For reservoir A, three samples were selected for gas–oil unsteady-state relative permeability testing. The samples were tested in the fresh state. For reservoir B, five samples were selected for gas–oil unsteady-state relative permeability testing. The samples were tested in the fresh state. During the displacement portion of the test, very high oil–water viscosity ratio exists within the core sample (higher than would be encountered in the reservoir). This high ratio is necessary to promote early breakthrough of the displacing phase and to prolong two-phase production. This technique results in a more accurate representation of the relative permeability relationship.

Humidified nitrogen was used as the displacing phase for this test. The nitrogen was humidified to prevent evaporation of the connate water within the core during the displacement. The oil and gas displaced from the core at constant pressure. Oil and gas production were monitored as a function of time. Relative permeability was calculated from the production data by using the theory developed by Buckley and Leverett [8] and extended by the Welge [9] equations, which related relative permeability to core end saturation.

2.2 Steady-State Water–Oil/Oil–Water Relative Permeability Tests

Steady-state methods yield the most reliable relative permeability data because capillary equilibrium is achieved in the method, fluid saturations can be measured directly, and the calculation procedure is based on the Darcy equation [5]. Because the equilibrium conditions must be attained at each saturation level, steady-state measurement requires many hours or even days to complete. Saraf and McCaffery [10] grouped the steady-state methods into four different categories. These are stationary fluid (static) method, capillary pressure (Hassler) method, dynamic (Penn-state) method and quasi-steady-state method.

The same samples were selected for water–oil steady-state relative permeability testing for reservoirs A and B to make data comparisons easier. Following measurement of the gas

displacing oil unsteady-state portion of the testing, the samples were flushed with oil to remove the nitrogen from the samples. To ensure that degassing of the samples was complete, a 450-psi back pressure was placed on the sample during this flush. Oil permeability at connate water saturation was compared to the same value obtained prior to the gas flood.

The steady-state method requires two fluids to be injected at constant flow rates and at a known ratio until the fluids come into capillary equilibrium with each other and the core material. High-pressure liquid chromatography pumps were used to inject the fluids. The equilibrium point was determined by monitoring the pressure drop across the core sample. Saturations were determined gravimetrically, using the density difference between the oil and water. Since the flow rate for each phase was known, as was the pressure drop across the core sample, effective permeability to each phase was determined. This procedure was carried out for the following ratios of water–oil:

100 % oil flow (Ko@ Scw)
1:10
1:5
1:1
5:1
10:1
100 % water flow (Kw@ Sor)

The procedure utilized in this study is summarized in the following steps:

- Reviewing the most common published relative permeability correlation models, which are presented in Section 3.
- Correlating between them and the available data sets.
- Determining the most applicable model.
- Predicting the parameters used in the most applicable model.
- Applying relative permeability data in determining some reservoir fluid properties.

3 Relative Permeability Correlation Models

Due to the importance of relative permeability in reservoir simulation, there is a dominant need to upscale it. Throughout the years, the researchers introduced several models that can be applied in the relative permeability modeling. Some of them were based on the capillary pressure measurement [11–14]. Other models did not require the capillary pressure measurements [1,15]. The following is a brief description of the models used in this study:

3.1 Corey (1954) Model

For the gas–oil relative permeability system, Corey [1] simplified the Burdine [12] model into the following relationships:

$$K_{\mathrm{rog}} = S_{\mathrm{oe}}^4 \tag{1}$$

$$K_{\mathrm{rg}} = (1 - S_{\mathrm{oe}})^2 (1 - S_{\mathrm{oe}}^2) \tag{2}$$

$$S_{\mathrm{oe}} = \frac{S_{\mathrm{o}} - S_{\mathrm{or}}}{1 - S_{\mathrm{or}}} \tag{3}$$

For the water–oil system, the Corey model has the following form:

$$K_{\mathrm{rw}} = S_{w}^{*4} \tag{4}$$

$$K_{\mathrm{row}} = (1 - S_{\mathrm{w}}^*)^2 (1 - S_{\mathrm{w}}^{*^2}) \tag{5}$$

$$S_{\mathrm{w}}^* = \frac{(S_{\mathrm{w}} - S_{\mathrm{wir}})}{(1 - S_{\mathrm{wir}})} \tag{6}$$

Wyllie and Gardner [16] proposed a set of equations to describe various types of rocks. In their work, they adopted the Corey model for the cemented sand and oolitic limestone.

Usually, the proposed exponents of Corey model did not meet the investigated data, and therefore, modification of Corey model was necessary to become:

For the wetting phase:

$$K_{\mathrm{rw}} = a(S_{\mathrm{w}}^*)^b \tag{7}$$

For nonwetting phase (K_{rnw}):

$$K_{\mathrm{rnw}} = c(1 - S_{\mathrm{rw}}^*)^2 (1 - S_{\mathrm{rw}}^{*d}) \tag{8}$$

where a, b, c and d are empirical constants, in which a and c constrain the relative permeability at saturation end points (S_{wir} and S_{or}). Thus, the relative permeability is controlled by the exponents b and d, in which the lower exponent values indicate heterogeneous rocks and higher values indicate homogenous rocks. More modification was carried out on Corey model to correlate the measured data. Ahmed [4] called it analytical equations:

For the oil–water systems:

$$K_{\mathrm{row}} = K_{\mathrm{ro}} @ S_{\mathrm{wc}} \left[\frac{1 - S_{\mathrm{w}} - S_{\mathrm{orw}}}{1 - S_{\mathrm{wc}} - S_{\mathrm{orw}}} \right]^{\mathrm{no}} \tag{9}$$

$$K_{\mathrm{rw}} = K_{\mathrm{rw}} @ S_{\mathrm{orw}} \left[\frac{S_{\mathrm{w}} - S_{\mathrm{wc}}}{1 - S_{\mathrm{wc}} - S_{\mathrm{orw}}} \right]^{\mathrm{nw}} \tag{10}$$

For the gas–oil systems:

$$K_{\mathrm{rog}} = K_{\mathrm{ro}} @ S_{\mathrm{gc}} \left[\frac{1 - S_{\mathrm{g}} - S_{\mathrm{wc}} - S_{\mathrm{org}}}{1 - S_{\mathrm{gc}} - S_{\mathrm{wc}} - S_{\mathrm{org}}} \right]^{ngo} \tag{11}$$

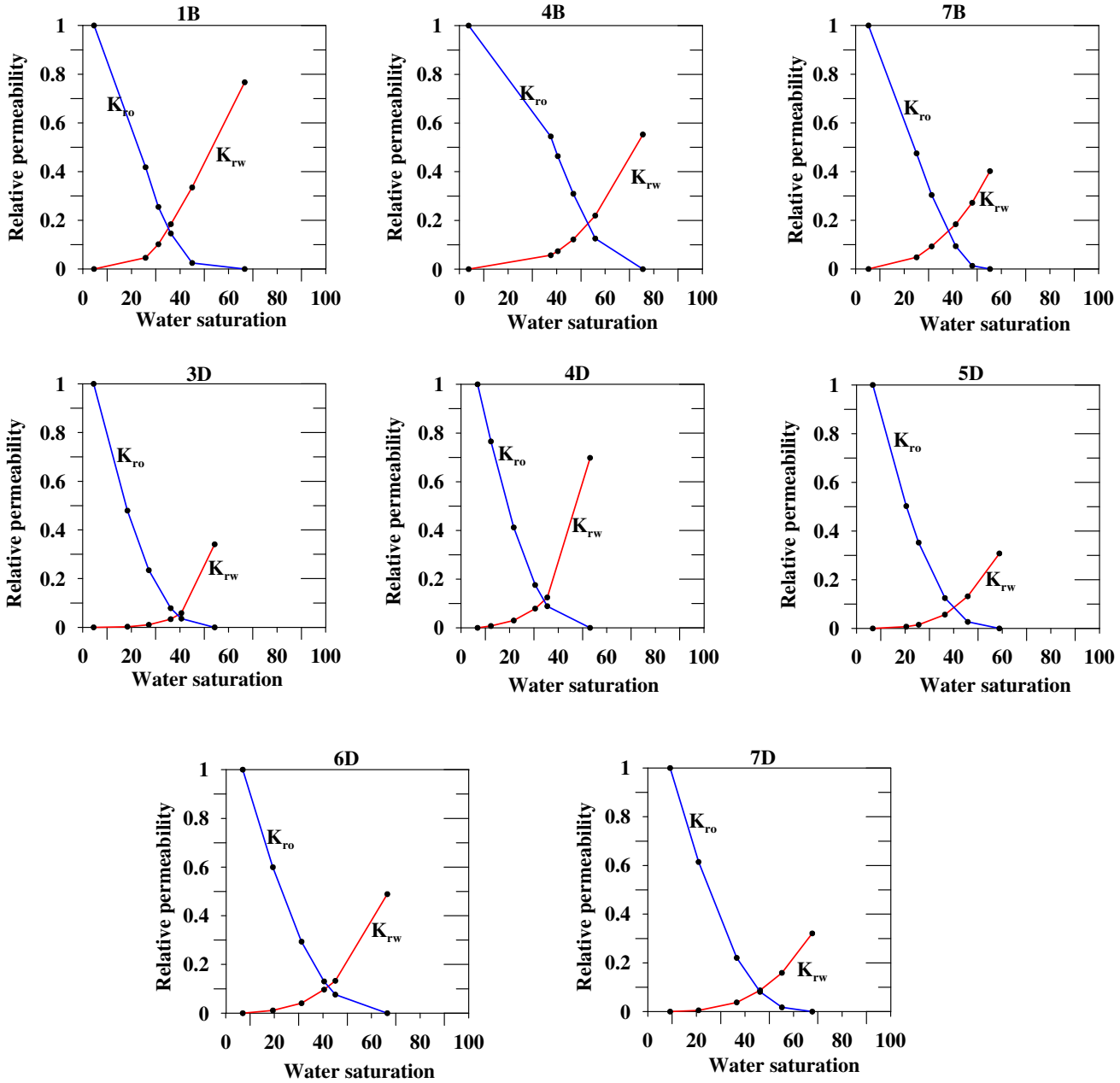

Fig. 2 Steady-state water–oil relative permeability showing rock wettability in both reservoirs based on when either curves crossing at $S_w > 50\,\%$ or $S_w < 50\,\%$. According to this method only 4B and 7D samples are water–wet

$$K_{rg} = K_{rg}@S_{org}\left[\frac{S_g - S_{gc}}{1 - S_{gc} - S_{wc} - S_{org}}\right]^{ng} \tag{12}$$

Based on the capillary pressure analysis, Brooks and Corey [13,14] modified the Corey [1] model by introducing a new parameter called pore size distribution (λ). Such parameter can be estimated from their proposed relation:

$$S_w^* = \left(\frac{P_c}{P_d}\right)^{\lambda} \tag{13}$$

where P_c = capillary pressure, psi
P_d = displacement pressure, psi
They replaced the Corey exponents by the following form:

$$K_{rw} = (S_w^*)^{(2+3\lambda)/\lambda} \tag{14}$$

$$K_{rnw} = (1 - S_w^*)^2(1 - S_w^{*(2+\lambda/\lambda)}) \tag{15}$$

It must be noted that, for $\lambda = 2$, the Brooks and Corey model will be reduced to Corey model. Recently, Li and Horne [17] and Li [18] used numerical simulation and fractal geometry

to introduce new approaches to upscale the capillary pressure and relative permeability, based on Corey and Brooks and Corey models. On the other hand, Li [19] used the resistivity index to calculate the relative permeability based on the Brooks and Corey model.

3.2 Pirson (1958) Model

For the wetting phase in both imbibition and drainage processes, Pirson [20] proposed the following equation:

$$K_{\mathrm{rw}} = \sqrt{S_{\mathrm{w}}^{*}}\, S_{\mathrm{w}}^{3} \tag{16}$$

For the nonwetting imbibition phase:

$$K_{\mathrm{rnw}} = \left[1 - \left(\frac{S_{\mathrm{w}} - S_{\mathrm{wc}}}{1 - S_{\mathrm{wc}} - S_{\mathrm{nw}}}\right)\right]^{2} \tag{17}$$

For the nonwetting drainage phase:

$$\mathrm{K_{rnw}} = (1 - S_{\mathrm{w}}^{*})\left[1 - (S_{\mathrm{w}}^{*})^{0.25}\sqrt{S_{\mathrm{w}}}\right]^{0.5} \tag{18}$$

3.3 Honarpour et al. (1982) Model

Honarpour et al. [15] introduced a set of empirical equations for the water–oil imbibitions of the relative permeability and gas–oil-drainage relative permeability from a large number of experimental data. For the sandstone and conglomerate, they proposed the following equations:

For water–wet reservoir:

$$K_{\mathrm{rw}} = 0.35388\left(\frac{S_{\mathrm{w}} - S_{\mathrm{wir}}}{1 - S_{\mathrm{wir}}}\right) - 0.010874\left[\frac{(S_{\mathrm{w}} - S_{\mathrm{wir}})}{(1 - S_{\mathrm{wir}} - S_{\mathrm{wor}})}\right]^{2.9} + 0.56556(S_{\mathrm{w}})^{3.6}(S_{\mathrm{w}} - S_{\mathrm{wir}}) \tag{19}$$

For intermediate wettability:

$$K_{\mathrm{rw}} = 1.5814\left[\frac{(S_{\mathrm{w}} - S_{\mathrm{wir}})}{(1 - S_{\mathrm{wir}})}\right]^{1.91} - 0.58617\left[\frac{(S_{\mathrm{w}} - S_{\mathrm{orw}})}{(1 - S_{\mathrm{wir}} - S_{\mathrm{orw}})}\right] \times (S_{\mathrm{w}} - S_{\mathrm{wir}}) - 1.2484\Phi(1 - S_{\mathrm{wir}})(S_{\mathrm{w}} - S_{\mathrm{wir}}) \tag{20}$$

For any wettability:

$$K_{\mathrm{row}} = 0.76067\left[\frac{(\frac{S_{\mathrm{o}}}{1-S_{\mathrm{wir}}}) - S_{\mathrm{or}}}{1 - S_{\mathrm{orw}}}\right]^{1.8}\left[\frac{S_{\mathrm{o}} - S_{\mathrm{orw}}}{1 - S_{\mathrm{wir}} - S_{\mathrm{orw}}}\right]^{2} + 2.6318\Phi(1 - S_{\mathrm{orw}})(S_{\mathrm{o}} - S_{\mathrm{orw}}) \tag{21}$$

$$K_{\mathrm{rog}} = 0.98372\left(\frac{S_{\mathrm{o}}}{1 - S_{\mathrm{wir}}}\right)^{4}\left[\frac{S_{\mathrm{o}} - S_{\mathrm{org}}}{1 - S_{\mathrm{wir}} - S_{\mathrm{org}}}\right]^{2} \tag{22}$$

$$K_{\mathrm{rg}} = 1.1072\left(\frac{S_{\mathrm{g}} - S_{\mathrm{gc}}}{1 - S_{\mathrm{wir}}}\right)^{2} K_{\mathrm{rg}}@S_{\mathrm{org}} + 2.7794\frac{S_{\mathrm{org}}(S_{\mathrm{g}} - S_{\mathrm{gc}})}{(1 - S_{\mathrm{wir}})} K_{\mathrm{rg}}@S_{\mathrm{org}} \tag{23}$$

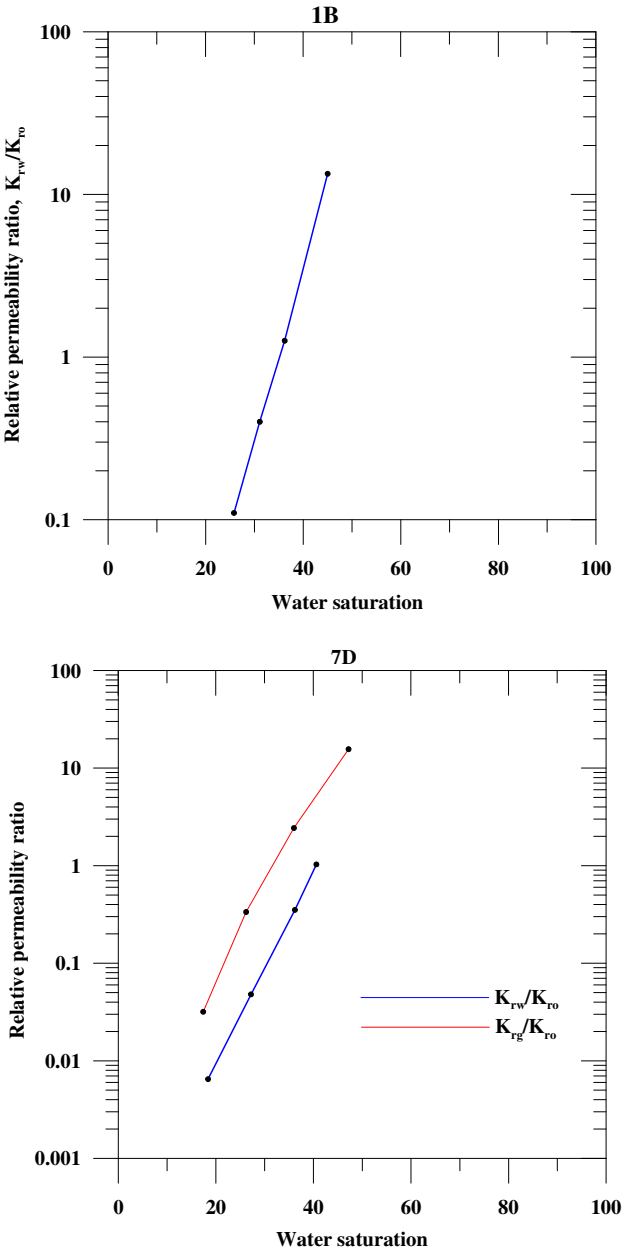

Fig. 3 Determination of rock wettability from the shape of the relative permeability ratio curve. *High value* for water–oil relative permeability ratio is preferential to oil–wet as in sample 1D. *Low value* for water–oil permeability ratio coupled with moving of gas–oil relative permeability ratio to over the water–oil relative permeability ratio argued for water–wet rock as in sample 7D

where Φ = porosity, fraction

3.4 Chierici (1984) Model

Chierici [21] upscaled the relative permeability curves of gas–oil-drainage system and water–oil imbibitions system. He proposed the following relations:

Table 2 Methods by which wettability can be determined

Sample no.	Methods				
	Curve shape (50 %> S_w <50 %)	Relative permeability ratio k_{rw}/k_{ro}	Connate water saturation	Ratio of $k_{rw}@S_{or}$	Shape of k_{rw} curve
1B	Oil–wet	Water–wet	Oil–wet	Oil–wet	Oil–wet
4B	Water–wet	Intermediate	Oil–wet	Oil–wet	Oil–wet
7B	Oil–wet	Water–wet	Oil–wet	Intermediate	Intermediate
3D	Oil–wet	Intermediate	Oil–wet	Intermediate	Intermediate
4D	Oil–wet	Oil–wet	Oil–wet	Oil–wet	Oil–wet
5D	Slightly Oil–wet	Intermediate	Oil–wet	Intermediate	Intermediate
6D	Slightly Oil–wet	Intermediate	Oil–wet	Intermediate	Intermediate
7D	Water–wet	Intermediate	Oil–wet	Intermediate	Intermediate

Table 3 Values of sum of squared error (SSE) for the studied models

Method	Reservoir	Samples	Sum of squared errors, SSE					
			Corey	Modified Corey	Practical	Pirson	Honarpour	Chierici
Unsteady state	A	1B	0.16	0.001	0.001	0.04	0.05	0.002
		4B	0.19	0.0005	0.0004	0.05	0.02	0.008
		7B	0.54	0.0005	0.0005	0.02	0.08	0.001
	B	3D	0.36	0.02	0.0004	0.115	0.44	0.16
		4D	0.24	0.018	0.0006	0.1	0.28	0.13
		5D	0.44	0.001	0.001	0.037	0.07	0.03
		6D	53	0.0009	0.0002	0.056	0.02	0.007
		7D	0.23	0.001	0.0008	0.017	0.05	0.01
Steady state	A	1B	0.56	0.02	0.008	0.25	0.07	0.02
		4B	0.07	0.01	0.01	0.08	0.09	0.01
		7B	0.36	0.005	0.003	0.06	0.12	0.54
	B	3D	0.36	0.01	0.0006	0.07	0.05	0.002
		4D	0.67	0.05	0.002	0.29	0.03	0.003
		5D	0.1	0.001	0.001	0.04	0.1	0.84
		6D	0.18	0.004	0.002	0.05	0.02	0.006
		7D	0.09	0.004	0.003	0.007	0.06	0.01

$$K_{rog} = e^{-AR_g^L} \tag{24}$$

$$K_{rg} = e^{-BR_g^{-M}} \tag{25}$$

where A, B, L and M are positive numbers, and R_g is the normalized saturation, which has the following correlation:

$$R_g = \frac{(S_g - S_{gc})}{(1 - S_{wir} - S_g)} \tag{26}$$

According to Feigl [6], it is better to apply the regression process to obtain the coefficients A, B, L and M on the logarithmic forms:

$$-\ln Kro = ARg^L \tag{27}$$

$$-\ln Krg = BRg^{-M} \tag{28}$$

For the water–oil imbibition system:

$$K_{ro}^* = e^{-AR_w^L} \tag{29}$$

$$K_{rw}^* = e^{-BR_w^{-M}} \tag{30}$$

where

$$R_w = \frac{S_w - S_{wir}}{1 - S_{or} - S_w} \tag{31}$$

$$K_{rw}^* = \frac{K_{rw}}{K_{rw}@S_{or}} \tag{32}$$

$$K_{ro}^* = \frac{K_{ro}}{K_{ro}@S_{wir}} \tag{33}$$

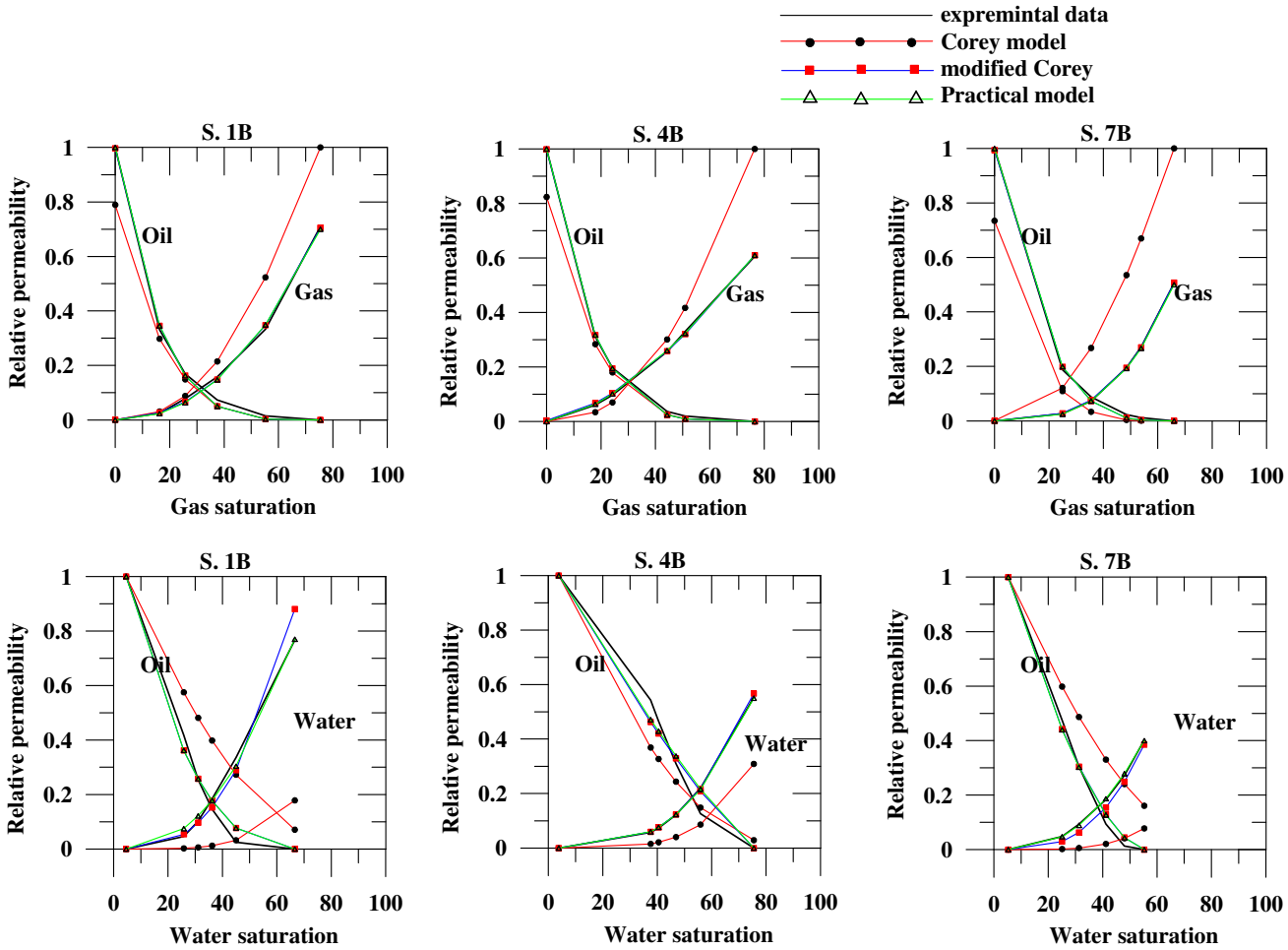

Fig. 4 Correlation between experimental data and the Corey (1954) model and its modified forms in reservoir A

4 Results and Discussion

Eight core samples were undergone laboratory tested for unsteady gas–oil relative permeability and steady water–oil relative permeability. Such data measurements were used to investigate the applicability of the previously mentioned relative permeability correlation models. The relative permeability curves belong to two consolidated microscopic heterogeneous sandstone reservoirs. The reservoir (A) includes three samples (1B, 4B and 7B) with different wettabilities (Fig. 2), according to the shapes of the relative permeability curves (either curves crossing at $S_w > 50\,\%$ or crossing at $S_w < 50\,\%$). Two samples (1B and 7B) are oil–wet, whereas the third sample (4B) is water–wet. For reservoir (B), which includes five samples (3D, 4D, 5D, 6D and 7D), three types of wettability can be noticed according to the previous parameter. It can be detected that two samples are oil–wet (3D and 4D), two samples are slightly oil–wet (5D and 6D), and the fifth sample is water–wet (7D). Identification of rock wettability is important to determine the behavior of the reservoir fluid production. In this concern, oil–wet reservoir is waterflood poorly, early water breakthrough, rapid increase in water cut and high residual oil saturation [3]. Another determination of wettability method was introduced by Mungan [22], based on the relative permeability ratio, in which if the entire curve is nearly vertical and extends over a small saturation interval, the rock is water–wet. On the other hand, the rock is oil–wet, when the relative permeability ratio curve has a gentle slope and extends over a longer saturation interval (Fig. 3). Involvement of gas–oil ratio and water–oil ratio was introduced by Raza et al. [23] to determine the rock wettability. They stated that moving of the gas–oil relative permeability ratio from under to over the water–oil relative permeability ratio indicates water wet rock (Fig. 3). Schneider and Owens [24] mentioned that in strongly water–wet, K_{rw} curves in water oil system show good agreement with K_{ro} curves in gas–oil system. Such condition was not encountered in the studied samples.

Another method was introduced by Treiber et al. [25], in which oil–wet formations tend to have lower connate water

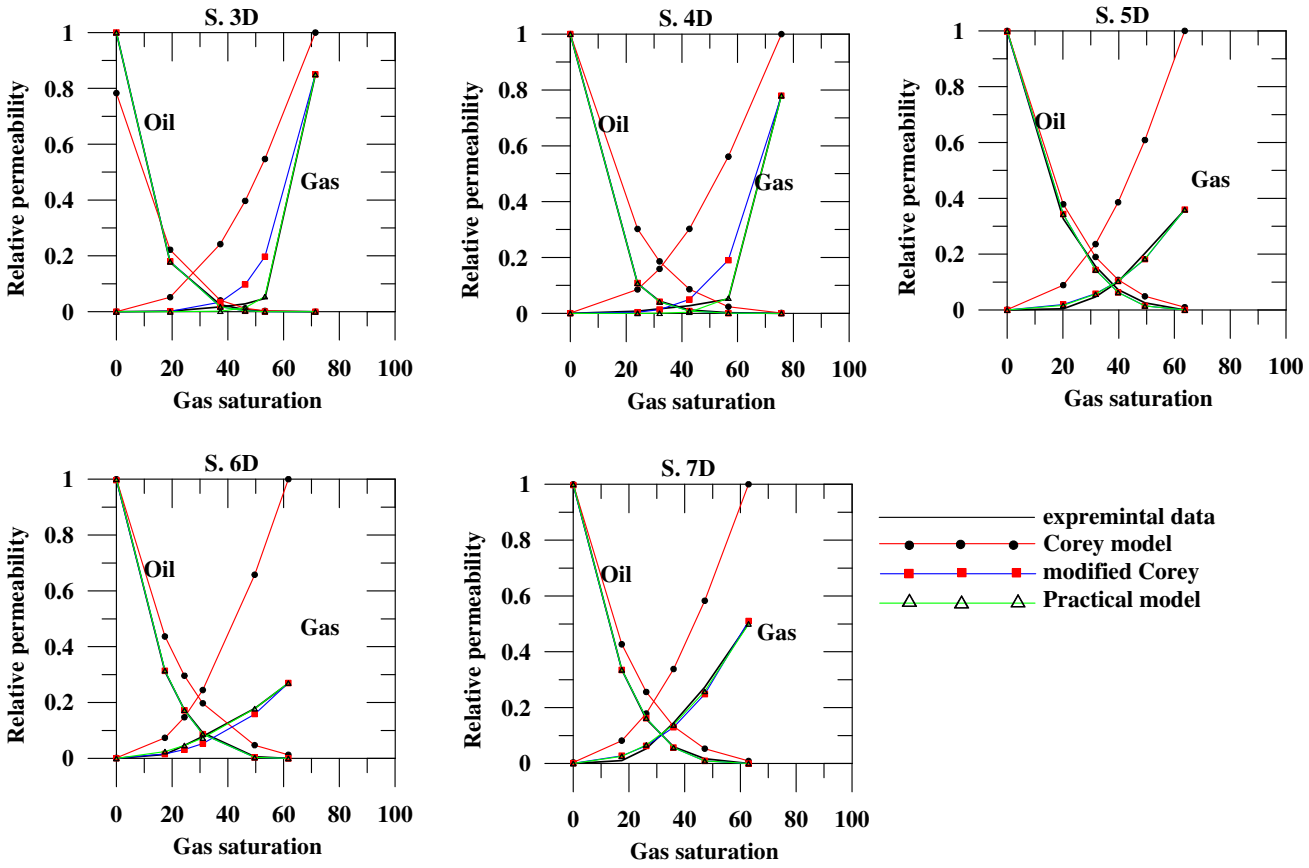

Fig. 5 Correlation between experimental data and the Corey (1954) model and its modified forms in reservoir B for gas–oil system

saturation than the water–wet ones. For oil–wet rocks, $S_{wir} < 0.1$ [26]. According to this parameter, all the studied samples are oil–wet. Another parameter used in the determination of wettability was introduced by Keelan [27], in which he used the ratio of water permeability at the residual oil saturation with the oil permeability at the connate water saturation. So, the water–wet system has a ratio < 0.3 and oil–wet system has a ratio > 0.5 [26]. Such parameter indicates oil–wet rock for the samples 1B and 4B in the reservoir (A), with intermediate wettability for sample 7B. For reservoir (B), the 4D sample is oil–wet, while the 5D and 7D samples are water–wet and the 3D and 6D samples are intermediate wettability rocks (Table 2). Confirmation of such conclusion can be inferred from the shape of the water relative permeability curve, in which Graig [28] concluded that water–wet systems have a water relative permeability less than 30 % at S_{orw}, while the oil–wet systems have a 50 % or higher water relative permeability at the residual oil saturation (Fig. 2).

To check the applicability of the previously mentioned relative permeability correlation models, they were classified into two groups. The first group involves Corey [1] model and its modified forms, and the second group involves the other models. For the first group, the results indicate good correlation with the modified and analytical equations. The lowest values of sum of squared errors were for practical and modified Corey models (Table 3). The Corey model fails to predict the relative permeability curves, especially for the nonwetting phase in both systems (Figs. 4, 5, 6). The analytical equations give results better than the modified Corey model in some cases. The exponents proposed by Corey showed considerable variation in modified and practical models. It can be noted that the samples 3D and 4D are considered the most homogenous rock studied samples, as inferred from the high b and d values.

For other models (Figs. 7, 8, 9), a deviation is observed, especially for Honarpour et al. [15] and Pirson [20] models. On the other hand, Chierici [21] model gives good correlation with the experimental data, practically in the reservoir A. In the reservoir B, this model fails to predict the saturation end points for both systems. So, we have good matching between the experimental data and the modified Corey, practical and Chierici models. The criterion between them depends on the number of parameters in each model, as well as the applicability to predict these parameters. For modified Corey model, it is needed to know the saturation end points (S_{wir} and S_{or}), in addition to the empirical constants; a, b, c and d that obtained

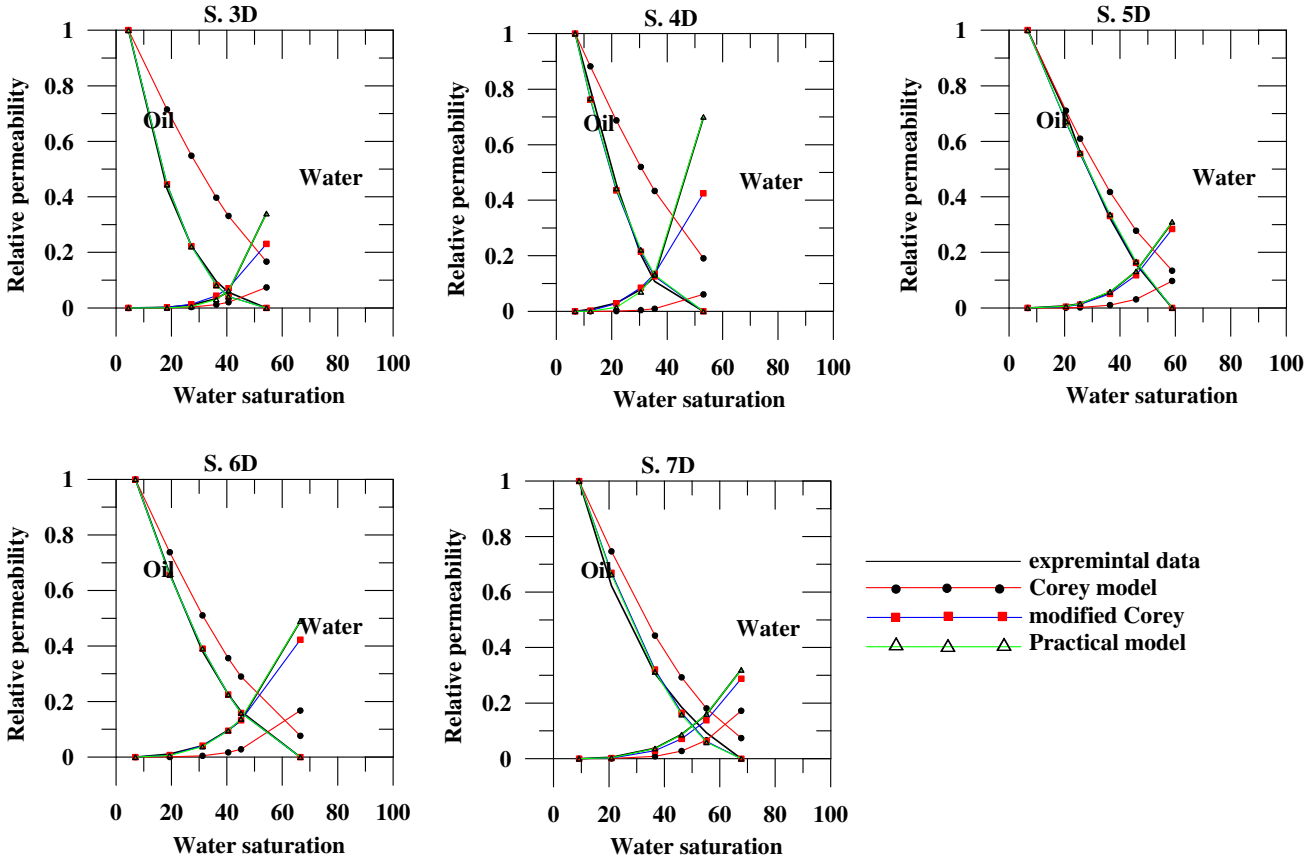

Fig. 6 Correlation between experimental data and the Corey (1954) model and its modified forms in reservoir B for water–oil system

from the fitting. Table (4) shows the values of empirical constants used in the modified Corey model to correlate the laboratory data. The variation in these constants from one sample to another is related principally to the degree of homogeneity of the rock samples. So, it can be concluded that the samples 3D and 4D are the most homogeneous which have the highest values for b and d empirical constants. Tables (5 and 6) show the empirical constants derived from the practical equation and Chierici model.

A good relationship exists between the porosity and residual oil saturation in the gas–oil system, in which the coefficient of determination, $r^2 = 0.76$. The relationship takes the following form:

$$S_{org} = 1.3\Phi^{0.96} \tag{34}$$

The relationships between the petrophysical parameters, such as porosity and permeability with S_{wir} and S_{orw}, show fair relationships with r^2 less than 0.6. Buryakovsky et al. [29] introduced a relationship between log permeability and S_{wir} in carbonate rocks. Applying this relationship on our data indicates poor correlation. Introducing the flow zone indicator (FZI) concept [30] resulted in a good correlation between permeability and S_{wir}, which translated into the following equation:

$$S_{\text{wir}} = 0.28FZI^{(-1.6FZI)} - 0.05 \quad \text{with } r^2 = 0.87 \tag{35}$$

This equation is based on 44 sandstone samples of different geologic ages and depositional environments. Averaging the values of saturation end points in both reservoirs resulted in the following equations:

For the gas–oil system

$$K_{\text{ro}} = 1.39S_{\text{w}}^{*3.95} \quad \text{with} \quad r^2 = 0.994 \tag{36}$$

$$K_{\text{rg}} = 0.734(1 - S_{\text{w}}^{*})^2(1 - sw^{*0.414}) \quad \text{with} \quad r^2 = 0.89 \tag{37}$$

For the water–oil system:

$$K_{\text{rw}} = 1.26S_{\text{w}}^{*2.19} \quad \text{with} \quad r^2 = 0.728 \tag{38}$$

$$K_{\text{ro}} = 1.05(1 - S_{\text{w}}^{*})^2(1 - S_{\text{w}}^{*1.18}) \quad \text{with} \quad r^2 = 0.905 \tag{39}$$

Plotting the predicted relative permeabilities as indicated from the Eqs. (36–39) against the laboratory data resulted in a good correlation, especially for the gas–oil system and the preferential water–wet rock samples (Figs. 10, 11).

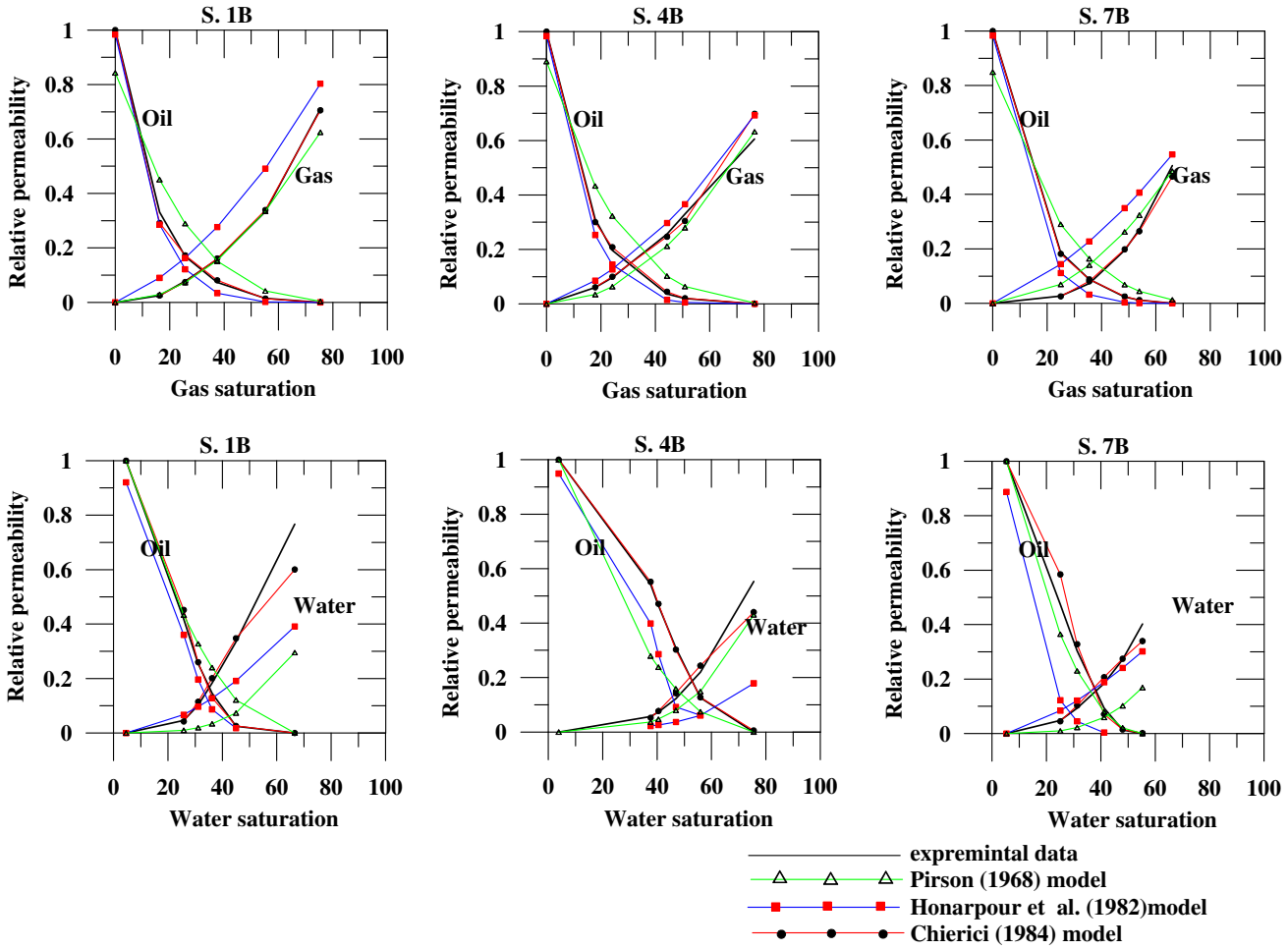

Fig. 7 Correlation between experimental data and the other models in reservoir A

One of the benefits of the relative permeability is aiding in the determination of water cut by using the following relationship based on Buckley and Leverett [8] work:

$$fw = \frac{1}{1 + \frac{1}{M}} \tag{40}$$

$$M = \frac{K_{\mathrm{rw}}}{K_{\mathrm{ro}}} \frac{\mu_{\mathrm{o}}}{\mu_{\mathrm{w}}} \tag{41}$$

Oil and water viscosities can be determined from the following equation series:

$$\mathrm{Log}(\log(\mu_{\mathrm{obd}} + 1) = 1.8653 - 0.025086\rho_{\mathrm{o}} - 0.5644 \log(T) \text{ [31]} \tag{42}$$

$$\mu_{\mathrm{od}} = A\mu_{\mathrm{obd}}^{B} \text{ [32]} \tag{43}$$

$$A = 10.175(R_{\mathrm{s}} + 150)^{-0.515} \tag{44}$$

$$B = 5.44(R_{\mathrm{s}} + 150)^{-0.338} \tag{45}$$

$$\mu_{\mathrm{o}} = \mu_{\mathrm{od}} \left(\frac{P}{P_{\mathrm{b}}}\right)^{m} \text{ [33]} \tag{46}$$

$$m = 2.6P^{1.187}\exp(-11.513 - 8.98(10)^{-5}P) \tag{47}$$

$$Rs = \gamma g \left[\left(\frac{P}{18.2} + 1.4\right) 10^{x}\right]^{1.2048} \text{ [34]} \tag{48}$$

in which

$$x = 0.0125\ \rho\mathrm{o} - 0.00091\mathrm{T} \tag{49}$$

$$\gamma g = \frac{\mathrm{Mw}}{28.96} \tag{50}$$

Based on the published data [35] and our calculations, the following results were obtained. The natural gas of reservoir A is composed of methane, ethane, propane, butane and N-butane with molecular weight equal to 17.5. Therefore, the specific gravity of the gas presented in the reservoir A based on Eq. 50 is 0.605. The measured oil density is 29 API [35]. From RFT log, reservoir pressure is 4750 psi and the reservoir temperature is 250 °F. So, the solubility gas–oil ratio (Rs) is equal to 723 SCF/STB. As a result, parameters A and B (Eqs. 44, 45) can be determined and consequently dead oil viscosity, which is equal to 3.061 cp. Therefore, the calculated reservoir oil viscosity based on Eq. 46 is 0.713 cp.

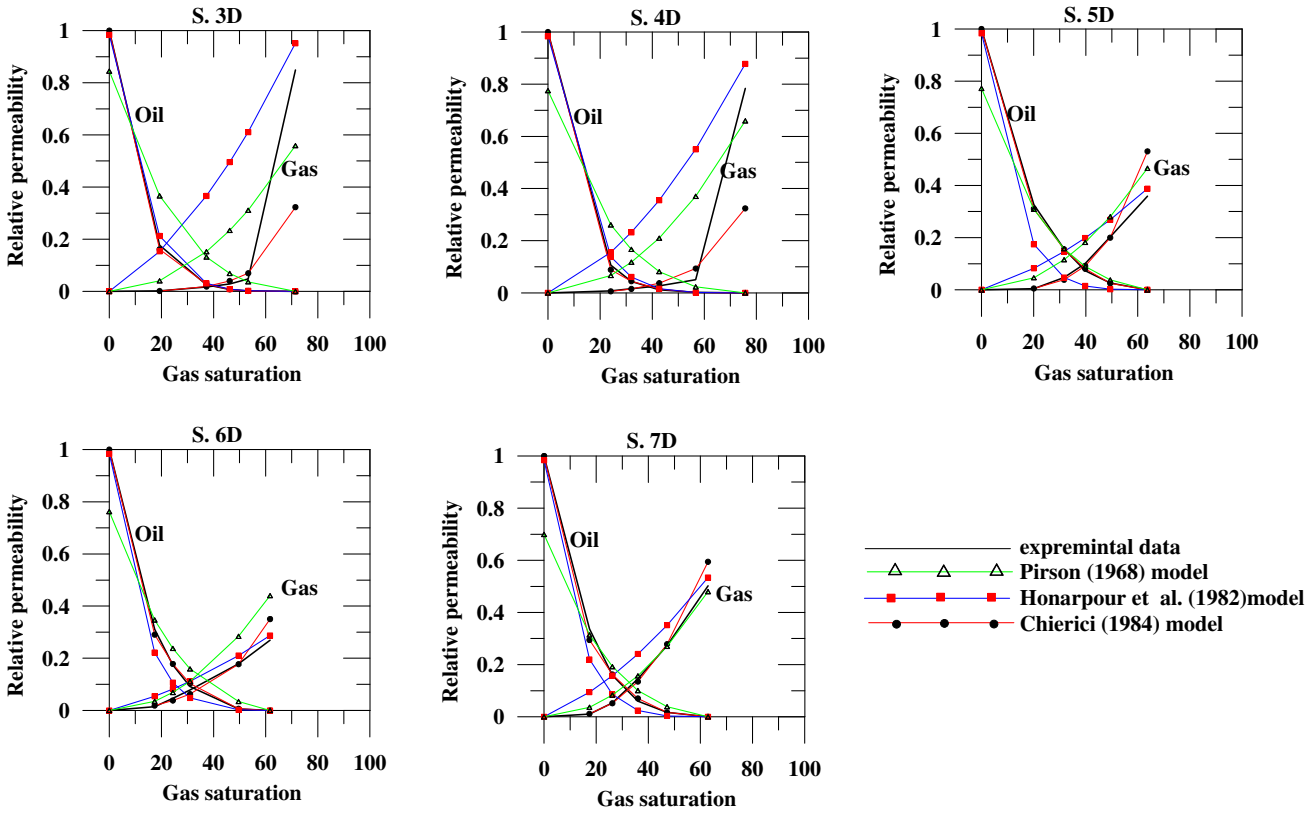

Fig. 8 Correlation between experimental data and the other models in reservoir B for gas–oil system

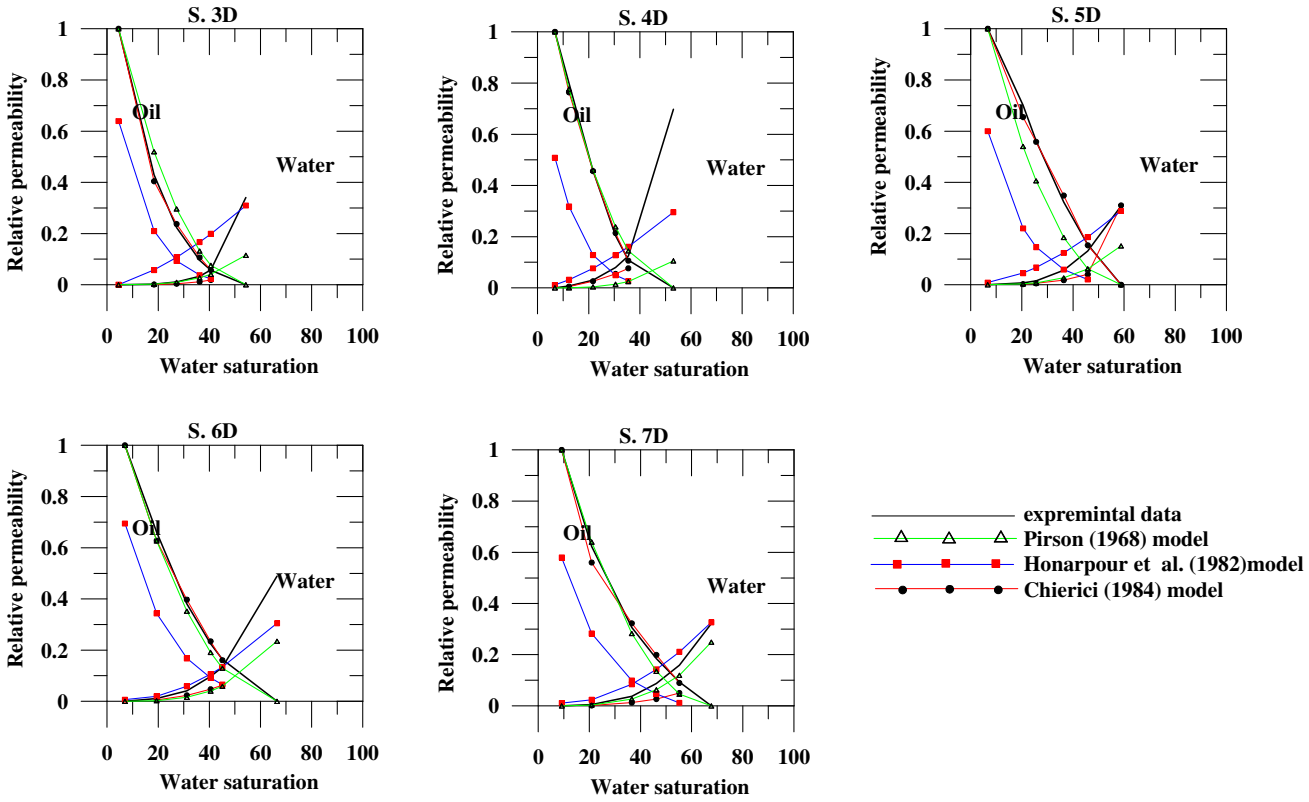

Fig. 9 Correlation between experimental data and the other models in reservoir B for water–oil system

Table 4 Modified Corey model parameters

Sample no.	Modified Corey model							
	Gas–oil system				Water–oil system			
	k_{rog}		k_{rg}		K_{rw}		k_{row}	
	a	b	c	d	a	b	c	d
1B	1.3	4.3	0.7	0.81	2.7	2.6	1	0.81
4B	1.2	4.3	0.6	0.56	1.4	3	1	0.4
7B	1.3	3.4	0.5	1.13	2.26	2.77	1	054
3D	1.4	5.45	0.85	3.36	2.5	3.6	1	0.8
4D	1.65	5.8	0.8	3.4	2.3	2.4	1	0.7
5D	1.3	2.8	0.36	1	1.7	3.1	1	0.4
6D	1.45	3.5	0.27	0.75	1.3	2.6	1	0.6
7D	1.6	3.4	0.5	0.9	1.1	3	1	0.6

Table 5 Practical equation parameters

Sample no.	Practical equations							
	Gas–oil system				Water–oil system			
	k_{rg}		k_{rog}		K_{rw}		k_{row}	
	$k_{rg}@S_{rg}$	ng	$K_{ro}@S_c$	ngo	$k_{rw}@S_{rw}$	nw	$k_{ro}@S_{wc}$	no
1B	0.7	2.2	1	4.36	0.77	2.17	1	2.4
4B	0.6	1.56	1	4.3	0.55	2.9	1	1.2
7B	0.5	3.1	1	3.4	0.4	2.3	1	1.6
3D	0.85	9.4	1	5.6	0.3	5.3	1	2.5
4D	0.8	9.2	1	5.8	0.7	3.4	1	2.1
5D	0.36	2.6	1	2.8	0.3	2.97	1	1.3
6D	0.27	1.9	1	3.5	0.5	2.85	1	1.8
7D	0.5	2.3	1	3.37	0.3	2.86	1	1.8

Table 6 Chierici (1984) model parameters

Sample no.	Chierici model							
	Gas–oil system				Water–oil system			
	k_{rg}		k_{rog}		K_{rw}		k_{row}	
	B	M	A	L	B	M	A	L
1B	1.7	0.56	2.7	0.57	0.51	1.7	10.1	2.37
4B	1.55	0.47	2.7	0.65	0.82	1.7	5.15	2.87
7B	2.16	0.67	2.8	0.63	1.08	1.37	6.4	2.68
3D	3.9	0.45	3.65	0.64	4.16	0.37	1.6	0.6
4D	3.4	0.46	4	0.58	2.6	0.32	1.5	0.85
5D	2.85	0.67	2.12	0.65	3.2	0.4	0.86	0.7
6D	2.56	0.41	2.6	0.69	2.6	0.41	1.2	0.71
7D	2	0.7	2.66	0.68	3.1	0.4	1.2	0.53

The reservoir water viscosity can be determined from charts [2,36] or from empirical equations [37]. The reservoir water viscosity is dependent mainly on the temperature, in which it decreases with increasing temperature. Salinity also has a slight influence. The following equation is used in this study to approximate reservoir water viscosity [38]:

$$\mu w1 = \mathrm{CT}^{\mathrm{D}} \tag{51}$$

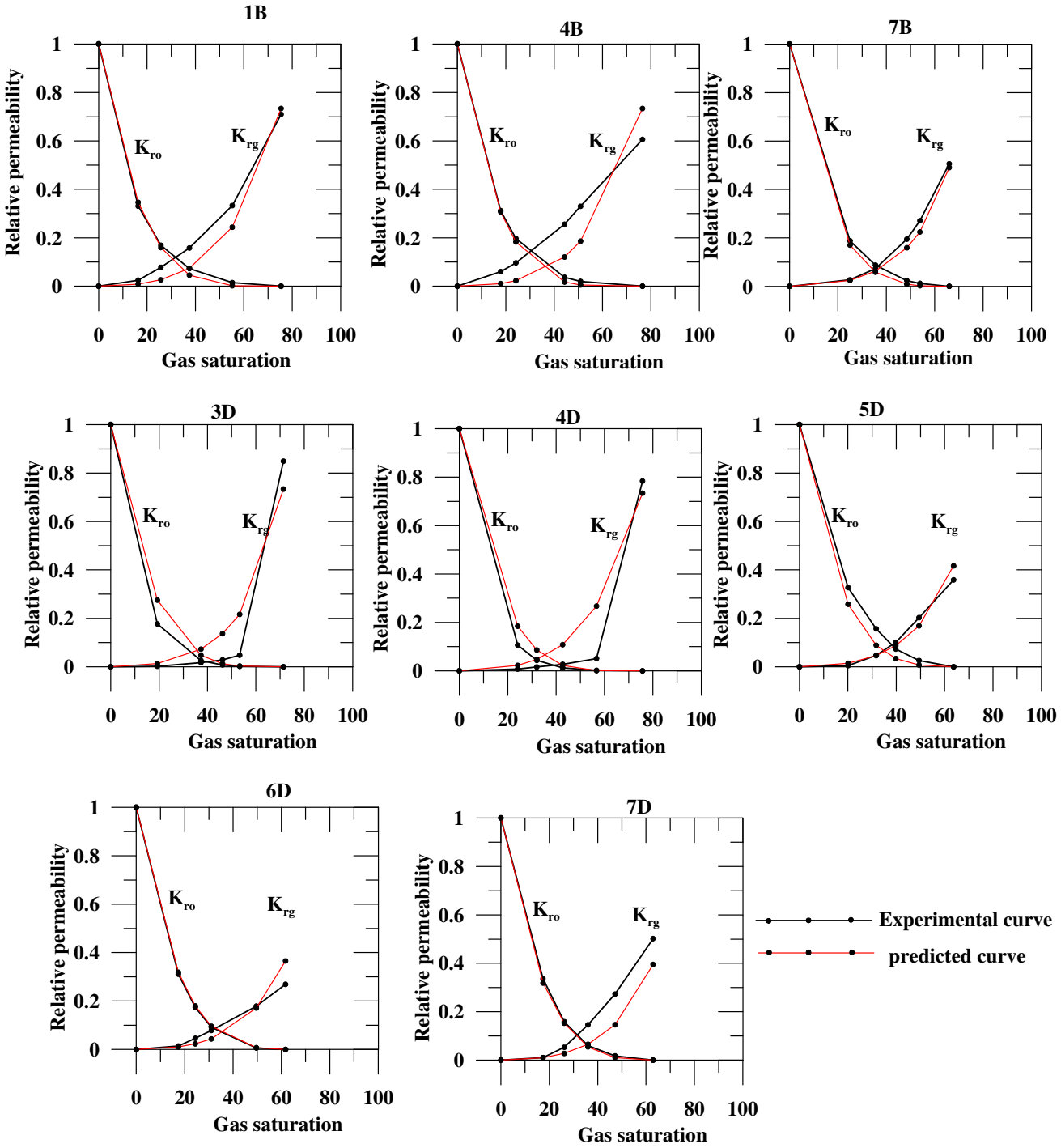

Fig. 10 Correlation between experimental data and the predicted curves using modified Corey model in both reservoirs in gas–oil system

where

$$C = 109.574 - 8.40564S + 0.313314S^2 + 8.72213^{*}10^{-3}S^3 \quad (52)$$

$$D = -1.12166 + 2.63951^{*}10^{-2}S - 6.79461^{*}10^{-4}S^2 - 5.47119 * 10^{-5}S^3 + 1.55586^{*}10^{-6}S^4 \quad (53)$$

According to McCain [38], Eq. (51) was found to be accurate to within 5 % over a temperature range from 100 to 400 °F and salinity up to 26 %.

With reservoir temperature of 256 °F, Eq. (51) yielded water viscosity of 0.44 cp. Therefore, the mobility ratio can be determined and consequently water cut. According to

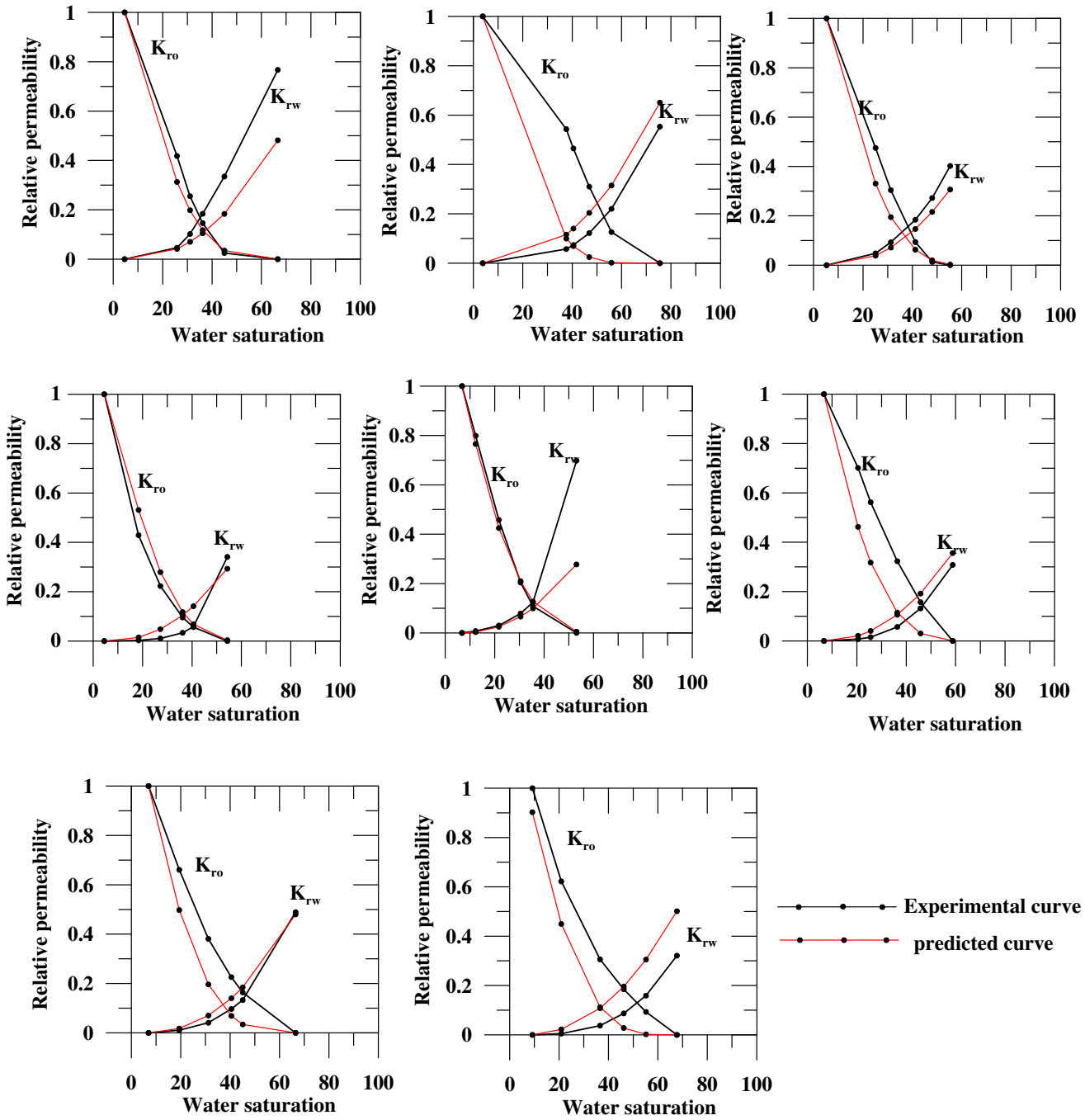

Fig. 11 Correlation between experimental data and the predicted curves using modified Corey model in both reservoirs in water–oil system

Warner [39], the mobility ratio can be determined at the relative permeability saturation end points as follows:

$$M = \frac{K_{\mathrm{rw}}@S_{\mathrm{orw}}}{K_{\mathrm{ro}}@S_{\mathrm{wi}}}\frac{\mu_{\mathrm{o}}}{\mu_{\mathrm{w}}} \tag{54}$$

The mobility ratio is favorable if $M < 1$, in which oil has mobility higher than water, or is unfavorable if $M > 1$, in which water has higher mobility than oil. The term $(\frac{\mu_{\mathrm{o}}}{\mu_{\mathrm{w}}})$ is equal to 1.6. Thus, the mobility ratio for reservoir A samples 1B, 4B and 7B is 1.2, 0.88 and 0.64, respectively. So, the mobility ratio is favorable for samples 4B and 7B and the reservoir quality increased from 1B to 7B. The water cut based on this method is 0.55, 0.46 and 0.39 for the three samples, respectively. Such results of water cut translate into water cutoff up to 54 % as estimated for sample 4B. On the other hand, mobility ratio is favorable for all reservoir B samples (Table 7).

Table 7 The studied reservoir properties

Reservoir	°F	Salinity, %	μ_o	μ_w	Sample	*M*	fw	Water cutoff
A	256	26	0.71	0.44	1B	1.2	0.55	0.38
					4B	0.88	0.46	0.55
					7B	0.64	0.39	0.38
B	225	25	0.58	0.49	3D	0.39	0.28	0.38
					4D	0.81	0.45	0.35
					5D	0.35	0.26	0.42
					6D	0.57	0.36	0.44
					7D	0.37	0.27	0.46

Table 8 Vertical sweep efficiency (E_V) based on Dykstra–Parsons [41] method, areal efficiency at breakthrough (E_{ABT}) and displacement efficiency (E_D) and overall waterflood oil-recovery efficiency (E_R) for the studied reservoirs

WOR	Vertical sweep efficiency, Ev							
	Reservoir A			Reservoir B				
	1B	4B	7B	3D	4D	5D	6D	7D
1	0.08	0.11	0.14	0.05	0.04	0.05	0.04	0.05
5	0.37	0.39	0.44	0.25	0.16	0.25	0.22	0.25
10	0.51	0.55	0.59	0.38	0.29	0.39	0.36	0.39
25	0.73	0.75	0.77	0.61	0.54	0.62	0.58	0.62
50	0.82	0.84	0.86	0.76	0.7	0.77	0.74	0.76
E_{ABT}	0.66	0.7	0.75	0.83	0.72	0.85	0.77	0.84
E_D	0.65	0.745	0.528	0.521	0.497	0.558	0.64	0.644
E_R at WOR = 50	0.352	0.438	0.34	0.329	0.25	0.365	0.365	0.411

The mobility ratio can be used to determine the areal efficiency at breakthrough (E_{ABT}) and the vertical sweep efficiency (E_v). Both areal and vertical sweep efficiencies and displacement efficiency (E_D) are used to determine the overall waterflood oil-recovery efficiency (E_R) as follows:

$$E_R = E_D^* E_A^* E_V \tag{55}$$

Displacement efficiency (E_D) can be used from the following equation:

$$E_D = \frac{(1 - S_{or} - S_{wir})}{(1 - S_{wir})} \tag{56}$$

Wilhite [40] introduced the following equation to calculate the areal efficiency:

$$E_{ABT} = 0.54602036 + \frac{0.03170817}{M} + \frac{0.30222997}{e^M} - 0.00509693M \tag{57}$$

The vertical sweep efficiency can be traditionally determined by using two methods. These methods are Stiles [42] and Dykstra and Parsons [41]. Two methods assume that the reservoir is composed of an idealized layered system. The layered system is selected based on the permeability ordering approach with layers arranged in order of descending permeability. Both methods required core permeability data.

Wilhite [40] method yielded areal efficiency equal to 0.66, 0.7 and 0.75 for the reservoir A samples 1B, 4B and 7B, respectively. Higher values were obtained for reservoir B (Table 8). Dykstra and Parsons [41] correlated the vertical sweep efficiency with the permeability variation "*V*," mobility ratio "M" and water–oil ratio "WOR" as expressed in bbl/bbl. For reservoir A, estimated permeability variation "*V*" from the routine core analysis is 0.85 (Fig. 12). Such value ($V = 0.85$) indicates an extremely heterogeneous reservoir. For reservoir B, permeability variation is reached 0.98. These high values of permeability variation resulted in low vertical sweep efficiency regardless the favorable mobility ratio. The results given by these methods are presented in Table 8 and Fig. 13.

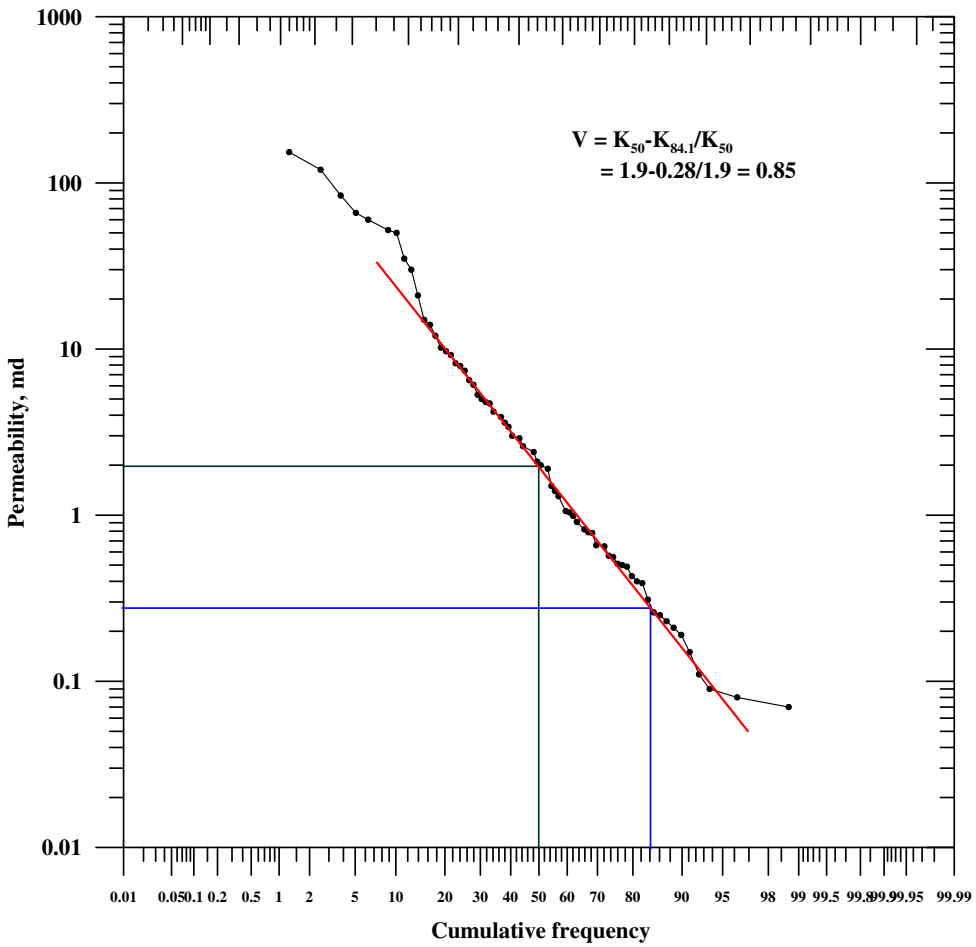

Fig. 12 Determination of permeability variation "*V*" as described by Dykstra and Parsons [41] indicates heterogeneous reservoir

5 Conclusions

From the previous results and discussion, it can be concluded that:

- Several correlation models were introduced to upscale the relative permeability.
- The most applicable model for the studied data sets was the practical and modified Corey models, which give the lowest sum of squared error values.
- Wettability of the studied samples shows some variation, according to the method of determination. In general, it ranged from water–wet to slightly-to-medium oil–wet.
- Relative permeability saturation end points were predicted by introducing empirical equations based on the flow zone indicator concept.
- Relative permeability can be used to aid in estimation of reservoir water cut, water cutoffs and overall waterflood oil-recovery efficiency.

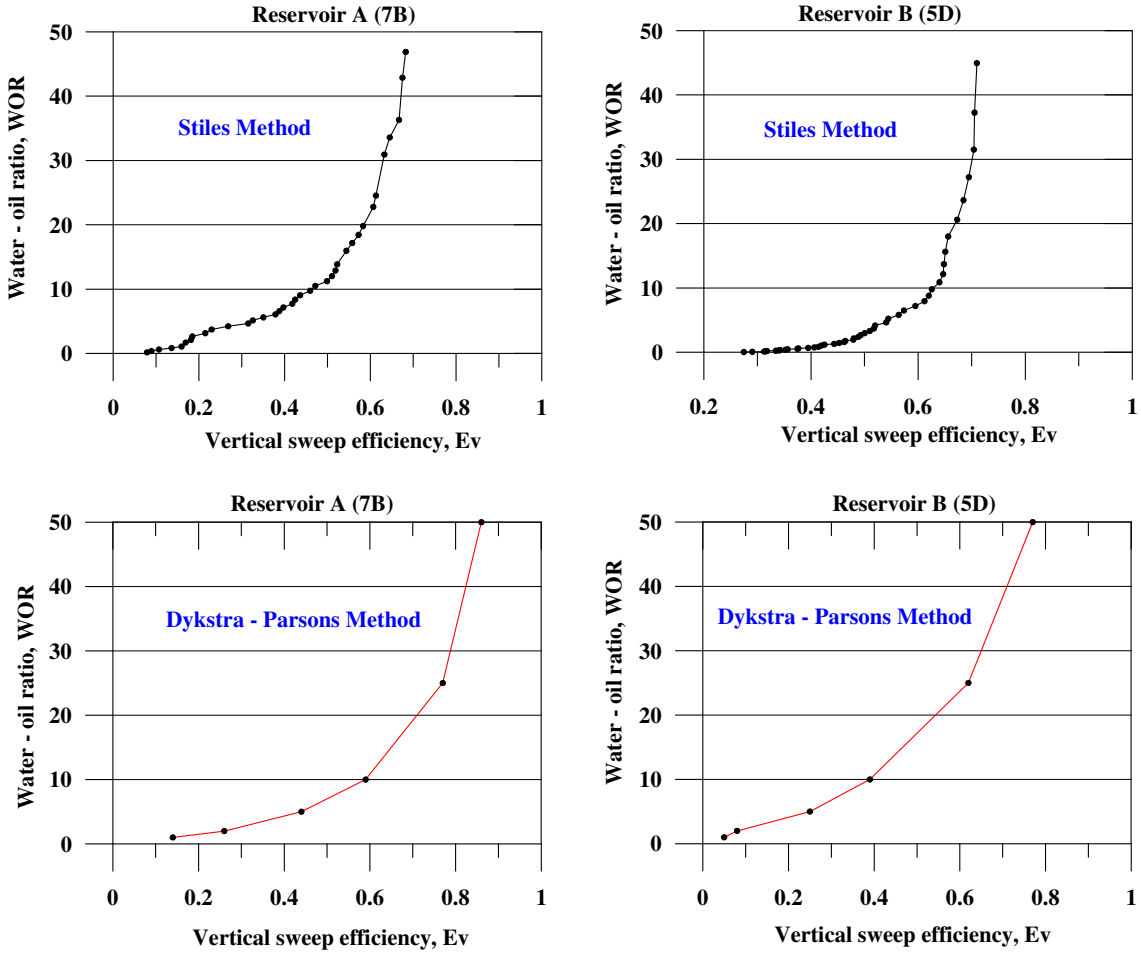

Fig. 13 Vertical sweep efficiency water–oil ratio as calculated using Stiles and Dykstra–Parsons methods for both reservoirs

Acknowledgments The author is grateful to the Egyptian General Petroleum Corporation (EGPC) and the Gulf of Suez Petroleum Company (GUPCO) for providing the data.

References

1. Corey, A.T.: The interrelation between gas and oil relative permeabilities. Prod. Mon. **19**, 38–41(1954)
2. Amyx, J.M.; Bass, D.M.; Whiting, R.: Petroleum Reservoir Engineering-Physical Properties. McGraw-Hill Book Company, New York (1960)
3. Honarpour, M.; Koederitz, L.; Harvey, A.H.: Relative Permeability of Petroleum Reservoirs. CRC, Boca Raton, Fla. (1986)
4. Ahmed, T.: Reservoir Engineering Handbook. 4th ed. Gulf Professional Publishing, Oxford (2010)
5. Ezekwe, N.: Petroleum Reservoir Engineering Practice. Prentice Hall, Boston (2011)
6. Feigl, A.: Treatment of relative permeabilities for application in hydrocarbon reservoir simulation model. NAFTA **62**, 233–243 (2011)
7. Ashrafi, M.: Experimental investigation of temperature dependency of relative permeability data in heavy oil systems with applications to thermal recovery. PhD, Norwegian University of Science and Technology (2013)
8. Buckley, S.E.; Leverett, M.C.: Mechanism of fluid displacement in sands. Trans. AIME **146**, 107–116 (1942)
9. Welge, H.J.: A simplified method for computing oil recovery by gas or water drive. Trans. AIME **195**, 91–98 (1952)
10. Saraf, D.N.; MaccCaffery, F.G.: Relative permeabilities. In: Donaldson, E.C.; Chilingarian, G.V.; Yen, T.F. Enhanced Oil Recovery, I Fundamentals and Analyses, Elsevier Publishing Company, New York (1985)
11. Purcell, W.R.: Capillary pressures—their measurement using mercury and the calculation of permeability therefrom. J. Pet. Technol. **1**, 39–48 (1949)
12. Burdine, N.T.: Relative permeability calculations from pore size distribution data. Trans. AIME **198**, 71–77 (1953)
13. Brooks, R.H.; Corey, A.T.: Hydraulic Properties of Porous Media. Colorado State University, Hydro 5, 27 p. (1964)
14. Brooks, R.H.; Corey, A.T.: Properties of porous media affecting fluid flow. J. Irrig. Drain. Div. **6**, 61–88 (1966)
15. Honarpour, M.M.; Koederitz, L.F.; Harvey, A.H.: Empirical equations for estimating two-phase relative permeability in consolidated rock. Trans. AIME. **273**, 2905–2908 (1982)
16. Wyllie, M.R.J.; Gardner, G.H.F.: The generalized Kozeny-Carmen equation—its application to problems of multi-phase flow in porous media. World Oil **146**, 210–213 (1958)
17. Li, K.; Horne, R.N.: Fractal characterization of the geysers rock. Proceedings of the GRC 2003 Annual Meeting. GRC Trans.27, 9 p. (2003)

18. Li, K.: Generalized capillary pressure and relative permeability model inferred from fractal characterization of porous media. SPE 89874, 10 p. (2004)
19. Li, K.: A new method for calculating two-phase relative permeability from resistivity data in porous media. Transp. Porous Med. **74**, 21–33 (2008)
20. Pirson, S.J.: Oil Reservoir Engineering. McGraw-Hill, New York (1958)
21. Chierici, G.L.: Novel relations for drainage and imbibition relative permeabilities. Soc. Pet. Eng. J. **24**(3), 275–276 (1984)
22. Mungan, N.: Enhanced oil recovery using water as a driving fluid. World Oil **3**, 77–83 (1981)
23. Raza, S.H.; Treiber, L.E.; Archer, D.L.: Wettability of reservoir rocks and its evaluation. Prod. Mon. **32**, 2–7 (1968)
24. Schneider, F.N., Owens, W.W.: Sandstone and carbonate two- and three-phase relative permeability characteristics. SPE, pp. 75-87 (1970)
25. Treiber, L.E.; Archer, D.L.; Owens, W.W.: A laboratory evaluation of the wettability of fifty oil-producing reservoirs. SPE **12**, 531–540 (1972)
26. Fanchi, J.R.: Integrated Flow Modeling. Elsevier Science B.V, Netherlands (2000)
27. Keelan, D.K.: A critical review of core analysis techniques. J. Con. Pet. Technol. **6**, 42–55 (1972)
28. Craig, F.F.Jr.: The reservoir engineering aspects of waterflooding monograph. New York. SPE of AIME (1971)
29. Buryakovsky, L.; Chilingar, G.V.; Rieke, H.H.; Shin, S.: Petrophysics Fundamentals of the Petrophysics of Oil and Gas Reservoirs. Scrivener Publishing, New Jersey (2012)
30. Amaefule, J.O.; Altunbay, M.; Tiab, D.; Kersey, D.G.; Keelan, D.K.: Enhanced reservoir description: using core and log data to identify hydraulic (flow) units and predict permeability in uncored intervals/wells. SPE **26436**, 205–220 (1993)
31. Egbogah, E.O.: An improved temperature—viscosity correlation for crude oil systems. The Annual Technical Meeting of the Petroleum Society of CIM, Banff, Alberta 83, pp. 34–32 (1983)
32. Beggs, H.D.; Robinson, J.R.: Estimating the viscosity of crude oil systems. JPT, pp. 1140–1141 (1975)
33. Vasquez, M.; Beggs, D.: Correlations for fluid physical properties prediction. JPT, pp. 968–970 (1980)
34. Beggs H.D.: Oil system correlations. In: Bradley, H.C. (ed.) Petroleum Engineering Handbook. SPE, Richardson, TX1 (1960)
35. Egyptian General Petroleum Corporation (EGPC): Gulf of Suez oil fields (A comprehensive overview) (1996)
36. Cosse, R.: Basics of Reservoir Engineering. Editions Technip, Paris (1993)
37. McCain, W.D. Jr.: The Properties of Petroleum Fluids 2nd ed. PennWell Publishing Co., Tulsa, OK (1998)
38. McCain, W.D. Jr.: The Properties of Petroleum Fluids 2 ed. PennWell Publishing Co., Tulsa, OK (1988)
39. Warner, H.R., Jr.: Waterflooding. In: Lake, L.W. (ed.) Petroleum Engineering Handbook: vol. V Reservoir Engineering and Petrophysics, pp. 1037-1102 (2007)
40. Willhite, G.P.: Waterflooding. Dallas: Society of Petroleum Engineers (1986)
41. Dykstra, H., Parsons, R.: The prediction of oil recovery by water flood. In: Secondary recovery of oil in the United States, 2nd ed. American Petroleum Institute, Washington, DC, pp.160–174 (1950)
42. Stiles, W.: Use of permeability distribution in waterflood calculations. Trans. AIME **186**, 9–13 (1949)